

Influence of Additives on the Electrodeposition of Zinc from a Deep Eutectic Solvent

Hasan F. Alesary ^{1,2}, Salih Cihangir ¹, Andrew D. Ballantyne ¹, Robert C. Harris ¹,
David P. Weston ³, Andrew P. Abbott ¹ and Karl S. Ryder * ¹

¹ Materials Centre, Department of Chemistry, University of Leicester, Leicester, UK LE1 7RH
k.s.ryder@le.ac.uk

² Department of Chemistry, College of Science, University of Karbala, Karbala, Iraq.

³ Department of Engineering, University of Leicester, Leicester, LE1 7RH, UK.

Abstract

The effects of nicotinic acid (NA), boric acid (BA) and benzoquinone (BQ) on the electrodeposition of Zn have been studied in a choline chloride (ChCl) ethylene glycol (EG) based deep eutectic solvent (DES), (1ChCl:2EG), and for the first time a bright zinc coating has been achieved when NA was used.

In metal electroplating processes, small-molecule additives are often included in the plating bath to improve properties of coating such as brightness, roughness, thickness, hardness and resistance to corrosion. The effects of additives on the electrodeposition of Zn from aqueous solution have been extensively investigated. However, very few studies have considered the effects of additives on the electrodeposition of Zn from ionic liquids or deep eutectic solvents. The electrochemical properties of the plating liquid have been studied here using cyclic voltammetry, chronocoulometry, chronoamperometry and microgravimetry (EQCM). Redox peak currents decrease when additives were included in the Zn solution and total charge was also reduced in experiments where additives were present. The Zn deposition being in good agreement with an instantaneous growth mechanism without additives changed to one of a progressive growth mechanism when additives were included in the coating bath. The current efficiency of zinc deposition in the DES without additives was 95%, which was reduced when additives were included. The resultant surface morphologies, thickness, topography, roughness and crystal structure of the Zn coating were revealed by scanning electron microscopy (SEM), atomic force microscopy (AFM) and X-ray diffraction (XRD), demonstrating that those additives serve as effective brighteners that can produce highly uniform and smooth zinc deposits.

Key Words

Electroplating, zinc, deep eutectic solvents, additives

Introduction

The electrodeposition of metal from ionic liquids (ILs) and deep eutectic solvents (DES) is an area that has received intense study; ^{1,2} however, relatively few studies have investigated the role of additives. ^{1,3} Zinc coatings are widely used in the field of corrosion-resistant coatings and energy storage. ^{4,5,6} Traditional zinc electrodeposition is usually performed in cyanide baths, acidic sulphate baths and acid chloride zinc baths. ^{4,7,8} The clear problem with these electrolytes, however, is that they are all both corrosive and highly toxic; furthermore, they all have a significant negative impact on the environment. Consequently, there is considerable interest in alternative electrolytes for zinc deposition.

Around ten years ago, deep eutectic solvents (DESs) were suggested as alternatives to classical room temperature ionic liquids, ^{9,10,11,12} as deep eutectic solvents, compared to ionic liquids, have excellent properties such as low cost, minimal toxicity, high metal solubility and are less sensitive to water. ^{10,11,13,14,15,16} DES media are proposed for various electrochemical applications such as metal electrodeposition. ¹⁷ Significant hydrogen evolution can result from the electrodeposition of metals from aqueous solutions. Hydrogen evolution, which is produced on the cathodic electrode surface, results in lowered current efficiency and often embrittlement. Given that hydrogen evolution and low current efficiency are clearly issues in the industrial plating of zinc, DESs could offer an attractive alternative for Zn plating that would allow these problems to be circumvented. ¹⁸

In this research, the effect of organic additives on Zn electrodeposition from deep eutectic solvents was investigated at 80°C. Different types of organic additives have been used in the electroplating of Zn from aqueous systems. It is extremely important to use these additives in the electrodeposition solvent due to their effect on the growth, morphology and structure of the resulting deposits. ¹⁹ They are normally added to the plating bath to improve properties of the electrodeposit, such as grain size, brightness, internal stress, hardness and resistance to corrosion. ^{19,20,21} However, whilst additives might promote such desirable properties, the detailed role they play in the electrodeposition process is often not clearly understood, hence rapid development in the field is inevitably hampered by the empirical nature of the associated research. ¹⁹ Researchers have suggested that additives can be adsorbed on the active side of the substrate and raise the activation

1 polarization of single ions, or otherwise that some additives act as inhibitors, or the
2 additives could be acting as complexing agents.¹⁹
3

4 Additives are normally high molecular weight polymeric organic compounds, such as
5 polyethoxylated compounds, which are used to produce bright Zn deposits from acidic
6 electrolytes.¹⁹ Alternatively, additives can be species that form colloidal suspensions,
7 which are more effective than small ions or single molecules. Organic additives that have
8 been used in Zn electroplating from aqueous solution include benzoic acid (BA),
9 polyethylene glycols (PEGs), *p*-benzoquinone (BQ) and boric acid (H₃BO₃).^{19,20} The
10 influence of additives on Zn electrodeposition from ionic liquids has also been studied.
11 Iwagishi studied the effects of ethylene glycol, 1,3-propanediol, 1,2-butanediol and 1,3-
12 butanediol on the electrodeposition of Zn from the Lewis base of liquid 1-ethyl-3-
13 methylimidazoliumbromide:ZnCl₂,^{22,23} demonstrating that the addition of each of these
14 species enhanced the current efficiency of the process, obtaining a smooth Zn deposit in
15 each case. Bright metal deposits were achieved from ILs when phenanthroline,
16 acetonitrile, ethylenediaminetetraacetic acid (EDTA) and sodium acetylacetonate were
17 added to the plating bath.²⁴ Endres *et al.*²⁵ showed that a brighter surface finish was
18 produced for Pd and Al-Mn alloys from the AlCl₃-1-butyl-3-methylimidazolium-chloride
19 IL when nicotinic acid was used as an additive. Recently, Liu *et al.* have studied zinc
20 electrodeposition from ionic liquids.²⁶ Chlorozincate ionic liquids were used for the
21 deposition of Zn.²⁷ The electrochemical potential windows of ILs are unusually wide
22 compared to those of aqueous electrolytes, therefore, ILs can be used in the
23 electrodeposition of Zn.
24
25
26
27
28
29
30
31
32
33
34
35
36
37
38
39
40

41 Five years ago, Xingwu Guo *et al.*²⁸ studied the effects of nicotinic acid on the
42 electrodeposition of Ni from deep eutectic solvents. They found that nicotinic acid was
43 able to produce a uniform smooth and bright Ni coating. Recently, we have studied the
44 effects of nicotinic acid, methylnicotinate boric acid and 5,5-dimethylhydantoin on the
45 electrodeposition of Ni from a choline chloride (ChCl) ethylene glycol (EG) based DES.
46
47
48
49
50
51
52
53
54
55
56
57
58
59
60
61
62
63
64
65

²⁹ This is a 1ChCl:2EG stoichiometry and is available under the commercial name *Ethaline*. It was interesting to note that bright mirror Ni coatings were produced as a result of using these additives.

The aim of the current study was to understand the effect of small molecule additives on the electrodeposition of Zn coatings from a DES electrolyte. Within this general area, the specific objectives were *i*) to study the behaviour of a small set of additives currently

1 used in aqueous electrolysis, *ii*) determine the effect on electrochemical parameters of
2 growth such current efficiency and nucleation / growth rate, *iii*) quantify the effect of
3 additives on physical parameters of the film such as surface roughness, structure. Here
4 we report the effects of three different additives (referred to as levellers and brighteners)
5 on the electrodeposition of Zn from a deep eutectic solvent (*Ethaline*). The additives tested
6 included nicotinic acid (NA), boric acid (BA) and *p*-benzoquinone (BQ). Properties of
7 zinc coating were found to be improved compared to the corresponding system without
8 additives, and for the first time a bright zinc coating has been achieved on a copper
9 substrate. These additives were chosen as a sample of those small molecule species that
10 are in common use as levellers and brighteners in our previous work (effect of nicotinic
11 acid, methylnicotinate boric acid and 5,5-dimethylhydantoin on the electrodeposition of
12 Ni from *Ethaline*). Cyclic voltammetry, chronocoulometry, chronoamperometry and the
13 quartz crystal microbalance were used to elucidate aspects of the Zn ion reduction with
14 these additives. The effect of those additives on morphology, thickness, roughness and
15 crystal structure of the Zn coating were also investigated.

30 **Experimental**

31 Choline chloride, [HOC₂H₄N(CH₃)₃Cl] (ChCl) (Aldrich 99%) was recrystallised from
32 absolute ethanol, filtered and dried under vacuum. Ethylene glycol (EG) (Aldrich +99%),
33 was used as received. Here, ethylene glycol (EG) is considered to be a hydrogen-bond
34 donor. The deep eutectic mixture was prepared by continuous stirring of the two
35 components at 60°C until a homogeneous, colourless liquid was formed. The zinc
36 chloride, ZnCl₂ (Aldrich ≥ 98 %), was used at a concentration of 0.4 M and 0.6 M. the
37 concentrations of additives used in the electrodeposition process were nicotinic acid (NA,
38 0.05 M) (Sigma ≥99.5 %), benzoquinone (BQ, 0.03 M) (Aldrich 98 %) and boric acid
39 (BA, 0.2 M) (Analar 99.8%) were all used as received.

40 Cyclic voltammetry, chronocoulometry and chronoamperometry were performed using
41 an Autolab PGSTAT12 potentiostat controlled by the GPES2 software (version 4.9). The
42 electrochemical cell consisted of three electrodes: a Pt disc (1 mm dia.) working
43 electrode, a Pt flag counter electrode and an Ag/AgCl reference electrode. Cyclic
44 voltammograms were recorded using a potential window of 0.0 to 1.5 V. In all
45 experiments, the working electrode was polished between each experiment with 0.05 μm

1 γ -alumina paste, washed with deionised water and then with acetone. Voltammograms
2 were carried out at the same temperature as the plating (typically 80 °C).
3

4 The data from the Quartz Crystal Microbalance (QCM) technique were recorded using a
5 Hewlett-Packard 87512A transmission/ reflectance unit via a 50 Ω coaxial cable, such
6 that the centre of the recorded spectra was close to the resonant frequency, f_0 , of the
7 crystal (ca. 10 MHz). To improve temporal resolution, the network analyser data
8 acquisition was controlled using a computer running the HP VEE software. This program
9 is capable of recording admittance spectra every 2-3 s.
10

11 In this work, a 10 MHz AT-cut polished (flat mirror) finish quartz crystal with a platinum
12 film thickness of 900 Å, deposited in a keyhole shape on both sides with central disc
13 active area of 0.23 cm², was used (International Crystal Manufacturing Co., Oklahoma
14 City, USA.). The crystal was placed in a Teflon cell such that one face of the crystal was
15 exposed to the solution and one face was exposed to air. The three-electrode
16 electrochemical cell was completed with a Pt flag counter electrode and an Ag/ AgCl
17 reference electrode. The measurements were performed at -1.25 V for Zn deposition at
18 80 °C.
19

20 The electrodepositions were achieved on a Cu substrate from *Ethaline* containing 0.4 M
21 ZnCl₂ in the presence and absence of additives. The cathode substrate was, firstly, etched
22 with an aqueous 0.87 M ammonium persulfate solution, (NH₄)₂S₂O₈ (Aldrich) and 0.2 M
23 H₂SO₄ (Fisher) solution, washed with water and then dried. The anode was Ti mesh, and
24 the electrodepositions were performed at 80°C and a current density of 3.3 mA cm⁻² for
25 2 h.
26

27 Scanning electron microscope (SEM) images were carried out using a Phillips XL30
28 ESEM instrument with an accelerator voltage of 20 keV, giving an average beam current
29 of ca. 120 μ A. Cross-section microstructure of the Zn coatings were mounted in a resin
30 using a Struers LaboPress 3. The samples were then polished first with 240 grit silicon
31 carbide paper to make them flat, then with diamond abrasives of successively 9 μ m and
32 3 μ m size and finally with a 0.05 μ m colloidal silica. Atomic force micrographs were
33 acquired using a Digital Instruments Nanoscope IV Dimension 300 (Veeco) atomic force
34 microscope with a 100 mm scanning head was used in both contact and tapping (resonant)
35 modes. The controlling software was Nanoscope version 6.13. Images were acquired in
36 air. Powder X-ray diffraction was performed using a Phillips model PW 1730 X-ray
37
38
39
40
41
42
43
44
45
46
47
48
49
50
51
52
53
54
55
56
57
58
59
60
61
62
63
64
65

1 generator, with a PW 1716 diffractometer and PW 1050/25 detector. The X-ray tube was
2 a long fine-focus Cu anode with Ni K α -filtered radiation of wave. It was typical operated
3 at 40 kV, 30 mA, and scanned between 15 and 110° 2 θ with a step size of 0.02° 2 θ . Angle
4 calibration was carried out using a synthetic Si sintered standard.
5
6
7
8
9

10 **Results and discussion**

11 **Effect of temperature on the voltammetric behaviour of Zn (II)**

12
13
14
15
16
17
18
19
20
21
22
23
24
25
26
27
28
29
30
31
32
33
34
35
36
37
38
39
40
41
42
43
44
45
46
47
48
49
50
51
52
53
54
55
56
57
58
59
60
61
62
63
64
65
Cyclic voltammetry of ZnCl₂ in *Ethaline* has been studied at room temperature and at
elevated temperature (80 °C). Fig. 1 shows a comparison of the cyclic voltammetry of
Ethaline containing 0.4 M ZnCl₂ at room temperature and at 80 °C; both experiments
were recorded at a scan rate of 30 mV s⁻¹. The cyclic voltammograms of ZnCl₂ recorded
at 80 °C differed significantly from those recorded at room temperature, showing a
dramatic increase in the Zn deposition and dissolution current peaks when performed at
80 °C. This was anticipated for various reasons: firstly, as temperature was increased,
the viscosity of the Zn electrolyte decreases, allowing an increase in the rate of mass
transport toward the electrodes. Secondly, the Zn electrolyte contains a high concentration
of Cl⁻ anions (*ca.* 5 M) which, through adsorption into the electrode surface, can impede
the approach of [ZnCl₄]²⁻ towards the electrode surface. As the temperature of the
electrolyte is increased, the number of adsorbed Cl⁻ anions on the electrode surface tends
to decrease, facilitating the approach of [ZnCl₄]²⁻ to the electrode surface and its
subsequent reduction.³⁰ From the cyclic voltammetry of ZnCl₂ (Fig. 1) it can be seen
that the rate electrodeposition of Zn from *Ethaline* at elevated temperature is considerably
improved over that at room temperature.

66 **Effect of additives on the voltammetric behaviour of Zn (II)**

67
68
69
70
71
72
73
74
75
76
77
78
79
80
81
82
83
84
85
86
87
88
89
90
91
92
93
94
95
96
97
98
99
100
As can be concluded from Fig. 1, the electrodeposition of Zn from *Ethaline* at 80 °C is
considerably better than at room temperature due to the increased efficiency and rate of
deposition of Zn. Therefore, in the subsequent electrodeposition of Zn from *Ethaline*
these conditions were selected. Fig. 2 shows the cyclic voltammetry of 0.4 M ZnCl₂ in
Ethaline at 80 °C in the absence and presence of different concentrations of the following
additives: (a) nicotinic acid (NA), (b) boric acid (BA), and (c) *p*-benzoquinone (BQ).

1 The cyclic voltammograms were recorded at a scan rate of 30 mVs⁻¹ using a 1.0 mm Pt
2 disc electrode, a Pt flag counter-electrode and an Ag/AgCl reference electrode. The
3 concentrations used were influenced by the work by Juma which in turn were limited by
4 solute solubility.³¹
5
6

7 In the absence of additive (Fig. 2), the onset of Zn²⁺ reduction (vs. Ag/AgCl) in *Ethaline*
8 is at E = -1.18 V and the oxidation of Zn occurs *via* a two-stage process, with two
9 oxidation peaks at E = -0.95 V and at -0.85 V. The two stripping peaks corresponded to
10 the presence of two energetically distinct phases of Zn. This was shown in previous
11 studies using solution phase and *ex-situ* electrochemical atomic force microscopy.^{32,33}
12 The deposition and stripping processes of Zn have been altered as a result of including
13 NA, as shown in Fig. 2 (a). A clear decrease in the magnitude of the reduction peak
14 currents can be seen with an increasing amount of NA in the electrolyte. In addition, a
15 negative shift of around 30 mV in the Zn²⁺ reduction potential occurred as NA was
16 introduced to the Zn electrolyte. The negative shift in the overpotential for the reduction
17 of Zn²⁺ can be attributed to the adsorption of NA on the electrode surface,^{28,34} thus
18 requiring additional energy to discharge the Zn²⁺ ions.
19
20
21
22
23
24
25
26
27
28
29

30 The adsorption of NA on different substrates has been confirmed in other studies by
31 Auger and SERS spectroscopy.^{28,35,36} NA can be adsorbed on the electrode surface
32 through the lone pair of electrons on either its nitrogen or oxygen atom, or both.^{36,37} NA
33 molecules can be absorbed on the surface in different ways, namely perpendicular or
34 parallel to the electrode surface, as shown in Fig. 3.
35
36
37
38
39

40 It can be seen from Fig. 2 (a) that the deposition and stripping peaks of Zn decreased
41 when 0.03 M NA was added to the Zn electrolyte. However, increasing the concentration
42 of NA results in an optimum concentration of NA at close to 0.05 M, Fig 2 (a). Further
43 increase in NA concentration results in a sustained decrease in current peak magnitude.
44 This behaviour could be related to the adsorption position of NA on the electrode surface.
45 The parallel adsorption position of NA on the electrode surface (as shown in Fig. 3) can
46 block a large area of the surface, and this may be more prevalent when a low
47 concentration of NA is present in the bath. Perpendicular NA adsorption could occur
48 when one increases the concentration of NA, where this orientation only blocks a small
49 area of the surface and thus allows for a relatively increased amount of Zn deposition. At
50 higher NA concentration the peak attenuation could be exacerbated by multi-layer
51 adsorption.
52
53
54
55
56
57
58
59
60
61
62
63
64
65

1
2
3
4
5
6
7
8
9
10
11
12
13
14
15
16
17
18
19
20
21
22
23
24
25
26
27
28
29
30
31
32
33
34
35
36
37
38
39
40
41
42
43
44
45
46
47
48
49
50
51
52
53
54
55
56
57
58
59
60
61
62
63
64
65

In contrast, both BA and BQ show sustained attenuation of the voltammetric peaks with increase in concentration of additive, Fig. 2 (b) and (c). An obvious decrease in the deposition of Zn occurred with an increasing concentration of BA, and a negative shift in the Zn reduction potential was also produced as a result of adding of BA to the Zn electrolyte. In aqueous electrodeposition, boric acid is often used to prevent an increase in pH at the cathodic electrode. However, it has been reported in the literature that that BA can be adsorbed onto the electrode surface.^{38,39} The behaviour of BA in DES is currently undetermined. However, a bright and smooth Zn deposit was achieved when BA was added to *Ethaline* containing a 0.4 M ZnCl₂ solution. Therefore, it is likely that the BA in the Zn bath could be absorbed onto the cathode surface and inhibit Zn deposition.

Voltammetric behaviour of additives in *Ethaline*

The electrochemical behaviour of NA, BA and BQ was examined by CV in neat electrolyte (*i.e.* in the absence of zinc salt), *Ethaline* at 80 °C. Fig. 4 shows the cyclic voltammetry of *Ethaline* in the absence and presence of NA, M BA and BQ at 80 °C on a Pt disk electrode (*vs.* an Ag/AgCl reference). Fig. 4 (a) demonstrates the cyclic voltammetry of *Ethaline* in the absence and presence of different concentrations of NA at 80 °C, where in the cyclic voltammetry of *Ethaline* a reduction peak was obtained at about -1.0 V. This peak corresponded to hydrogen evolution, but is shifted positively by 20 mV at a concentration of 0.05 M NA in the electrolyte. The shift and the increase in the reduction peak corresponded to an increase in hydrogen evolution. In Fig. 4 (a), a small reduction peak can be seen at about -0.5 V, which is associated with the reduction of NA. From Fig. 2 (a) and Fig. 4 (a), the onset potential of 0.4 M Zn without NA is more negative in comparison to the onset potential of NA in *Ethaline* by -0.5 V. This suggests that NA has been reduced and blocks the active points of the surface before Zn deposition. As a consequence of these differences in the potential, the cathodic reaction is more likely to be inhibited. It has been reported that voltammograms of NA dissolved in a pH 5.0 phosphate buffer saline on a polycrystalline gold electrode appear at a more positive potential.⁴⁰ However, the cathodic peak is twice as high as the anodic peak current.

1
2
3
4
5
6
7
8
9
10
11
12
13
14
15
16
17
18
19
20
21
22
23
24
25
26
27
28
29
30
31
32
33
34
35
36
37
38
39
40
41
42
43
44
45
46
47
48
49
50
51
52
53
54
55
56
57
58
59
60
61
62
63
64
65

As we have been using BA as a brightener in the electrodeposition of Zn from *Ethaline*, it is necessary to study the electrochemical behaviour of BA itself in *Ethaline*. Fig. 4 (b) shows the cyclic voltammograms of different concentrations of BA in *Ethaline* at 80°C. There is a clear new cathodic peak that has started to appear at about -0.5 V as BA was introduced into the electrolyte, whose intensity increases with an increasing concentration of BA. Boric acid could be dissociated in *Ethaline* to form the $[H_2BO_3]^-$ anion and H^+ . Therefore, the peak that started to appear at -0.5 V could specifically correspond to the adsorption of BA on the Pt electrode surface that then reduces with the consequent evolution of hydrogen, or this peak could otherwise be attributed to the adsorption of dihydrogen borate on the electrode surface via a one-electron transfer reaction. EI-Shafei and Aramata reported that BA can be adsorbed on a Pt (111) surface in acidic aqueous solutions.^{41,42} They found that the specific adsorption of BA takes place at more positive potentials. This is could be due to the effect of the natural electrolyte and electrode substrate. Thus, from the voltammetry of BA in *Ethaline*, as shown in Fig. 4 (b), it can be suggested that BA is adsorbed on the electrode surface and inhibits Zn deposition.

Fig. 4 (c) shows the cyclic voltammograms recorded for different concentrations of BQ in *Ethaline* at 80°C. Significant changes have occurred in the cyclic voltammograms of *Ethaline* through the use of BQ. The onset of cathodic reduction for *Ethaline* was at -0.9 V. However, using BQ, the onset of cathodic reduction was shown to occur at about -0.1 V where this corresponds to the reduction of BQ. As has been shown previously, Zn can be deposited in *Ethaline* at -1.18 V. Thus, it can be said that BQ adsorbs on the electrode surface and blocks the active sides before deposition of Zn.

Chronocoulometry

Chronocoulometry (CC) data in the form of integrated Cottrell plots provide information regarding the reaction process and can be used to determine if a reaction is under mass-transport or kinetic control.⁴³ For example we have recently examined the chronocoulometry of 0.01 M $CuCl_2 \cdot 2H_2O$ in *Ethaline* using a Pt disc electrode, and found that metal growth was diffusion controlled.¹⁷

In the current study, Zn chronocoulometry experiments were performed on a Pt disc electrode from *Ethaline* containing 0.4 M $ZnCl_2$ at 80°C in the absence and presence of 0.05 M nicotinic acid, 0.15 M boric acid and 0.03 M *p*-benzoquinone, as shown in Fig.

5, where all experiments were performed for potential steps from 0.0 V (held for 10 s) to -1.3 V for 30 min. Fig. 5 shows the plots of charge vs. $t^{1/2}$ are not linear suggesting that the processes are not controlled by diffusion. It is clear from Fig. 5 that the charge (Q) for Zn deposition in the presence of additives decreased. This indicates that electrodeposition of Zn from an additive-free system is faster than in a system containing additives; the same conclusion was drawn from the results of our cyclic voltammetry. According to Faraday's Law ($Q = nFN$), the charge measured is directly proportional to the number of species deposited in moles (N). This means that current efficiency of Zn deposition from *Ethaline* in the presence of additives will be less than the efficiency of Zn deposition from an additive-free electrolyte. The current efficiencies of Zn electrodeposition from *Ethaline* in the absence and presence of these additives were investigated using a quartz crystal microbalance (QCM), which will be discussed later.

Nucleation mechanisms

In order to further probe the possible change in the mechanism of Zn reduction, the nucleation mechanism needs to be investigated. Therefore, the chronoamperometry method was used to study the nucleation mechanism of Zn deposition. The chronoamperometric study was performed using a potential between -0.50 V to -1.25 V with a polished Pt disk vs. Ag/AgCl.

To identify trends in nucleation mechanisms of metal electrodeposition, a number of methods have been devised, the most widely used being the model developed by Scharifker and Hills,⁴⁴ which allows chronoamperometric data to be assigned to one of two limiting nucleation mechanisms, instantaneous or progressive. In an instantaneous nucleation process, the model assumes the rate of nucleation is high and that coverage of all active sites by nuclei is essentially instantaneous. This process is described by Equ. 1:

$$\left(\frac{i}{i_m}\right)^2 = \frac{1.9542}{t_m} \left\{1 - \exp\left[-1.2654 \left(\frac{t}{t_m}\right)\right]\right\}^2 \quad \text{Equation 1.}$$

In the progressive nucleation mechanism, the rapid growth of a large number of active sites is achieved throughout the reduction, a process which is described by Equ. 2:

$$\left(\frac{i}{i_m}\right)^2 = \frac{1.2254}{\frac{t}{t_m}} \left\{1 - \exp\left[-2.3367 \left(\frac{t}{t_m}\right)\right]^2\right\}^2 \quad \text{Equation 2}$$

In both processes, i_m is the maximum current density and t_m is the time taken to achieve i_m . Fig. 6 shows the normalised i - t curves associated with the theoretical models for three-dimensional instantaneous and progressive nucleation as well as the experimental data for Zn deposited from *Ethaline* at 80°C in the absence and the presence of additives: (a) without additives, (b) 0.05 M NA, (c) 0.15 M BA and (d) 0.03 M BQ. When the overpotential is applied, the current initially rises quite sharply due to double layer charging, followed by a relaxation in current. A subsequent rise to the current maximum, indicative of a nucleation process, is then observed. This current increase is proposed by Scharifker and Hills to be caused by the formation and growth of nuclei. As the individual nuclei growth zones begin to overlap, the current falls to a level indicative of a diffusion-limited process.

The nucleation mechanism for Zn deposition on a Pt electrode from *Ethaline* without additives using the Scharifker-Hills model is shown in Fig. 6 (a), where the nucleation mechanism fits quite well to that of a progressive growth process. However, at times beyond the current maximum, (i/i_m), the experimental data do not fit well to either model². The nucleation mechanism of Zn in the presence of NA and BA in *Ethaline* is shown in Fig. 6 (b) and (c), respectively, where the mechanism fits well with one describing progressive growth. The nucleation mechanism of Zn deposition in the presence of BQ also suggested a progressive growth mechanism in the early phases but fits better to an instantaneous growth model after a long period of time, as is clear in Fig. 6 (d). This suggests that with increasing induction time, the electrode surface is subject to a considerable blocking effect by additives. A transition between the two nucleation mechanisms has been reported for nucleation and growth processes controlled by mass transfer.^{19,45,46,47}

Gravimetric analysis

In addition to the cyclic voltammetry, chronocoulometry and chronoamperometry, the Electrochemical Quartz Crystal Microbalance (EQCM) technique has been used to study

1 the effect of NA, BA and BQ on current efficiency of Zn deposition from *Ethaline*. The
2 QCM technique uses a resonant quartz crystal, where this crystal is used as a mass probe
3 for the electrolytic deposition of the metal. The consequent change in resonant frequency
4 of the quartz crystal corresponds to the mass of metal deposited. In this case the
5 frequency data were derived from acoustic impedance spectra acquired during deposition.
6 This methodology was adopted in order to rule out viscoelastic effects during deposition.
7 Subsequently frequency data were converted into mass changes using the Sauerbrey
8 equation.⁴⁸ The data regarding the effect of the addition of 0.05 M NA, 0.15 M BA and
9 0.03 M BQ on the growth of Zn from *Ethaline* at 80°C are shown in Fig. 7.

10
11
12
13
14
15
16
17 The mass- charge data shown in Fig 7 are quite noisy and this is because of the low
18 resonant amplitude of the quartz crystal in the DES media caused by the relatively high
19 viscosity (*ca* 40 cP at room temp.) Despite this, there are clear differences in the data for
20 Zn deposition with and without the additives. In all the data sets (Fig. 7) there is a period
21 at the beginning of the experiment where charge is passed but very little measured mass
22 results. This is indicative of an induction period and can often be attributed to a substrate
23 effect. Once the substrate is covered with depositing metal (here Zn) then subsequent
24 deposition is more effective. The current efficiencies are calculated from the slope of the
25 mass-charge plots using Faraday's law and these data are presented in Table 1.

26
27
28
29
30
31
32
33
34 Fig. 7 shows the mass/charge traces for electrodeposition of Zn from *Ethaline* in the
35 presence and absence of additives. From Fig. 7, the current efficiencies of Zn depositions
36 from *Ethaline* in the presence and absence of 0.05 M NA, 0.15 M BA and 0.03 M BQ at
37 80°C were measured. Metallic Zn was deposited on a Pt-coated resonant quartz crystal
38 under a constant potential of -1.3 V from *Ethaline*-based liquids containing 0.4 M ZnCl₂
39 at 80°C in the absence of additives.

40
41
42
43
44
45
46
47
48
49
50
51
52
53
54
55
56
57
58
59
60
61
62
63
64
65
The current efficiency for Zn deposition in the absence of additive is close to unity at
91%. Addition of BA significantly reduces the current efficiency to 71% and this is
accentuated with addition of NA which gives the lowest current efficacy at 52%. The
effect of reducing current efficiency for these additives is almost certainly due to proton
reduction. Given that the NA concentration is significantly lower than the BA
concentration in these experiments, these data tend to indicate that NA is a stronger acid
in this DES medium. Addition of BQ does not have this effect because there are no labile,
reducible protons available. The current efficiency observed for Zn deposition in the
presence of BQ is 95% and very similar to Zn without additives. Given the noise levels

1 present in the data (Fig. 7) the difference between these two numbers lies within the
2 resolution of the measurement.
3
4
5

6 **Zinc deposit morphology** 7

8 Photographs, morphologies and cross-sections of Zn deposits that have been obtained
9 from *Ethaline* with a concentration of 0.4 M ZnCl₂ in the presence and absence of NA,
10 BA and BQ are shown in Fig. 8. All Zn electrodepositions were achieved on Cu
11 substrates at 80°C for 2 h at a current density of 3.3 mA cm⁻². Fig. 8 (a) shows the
12 morphology of the Zn deposit that was obtained from an additive-free electrolyte, where
13 it can be seen that different-sized Zn particles were obtained with a rough, polycrystalline
14 morphology. Clear changes in the morphologies of the Zn deposit occurred when NA
15 Fig. 8 (b), BA Fig. 8 (c) and BQ Fig. 8 (d), were added individually to the Zn electrolyte.
16
17

18 In previous work, the effects of nicotinic acid on the electrodeposition of Ni (II) from
19 DES were investigated. It was found that nicotinic acid inhibited Ni deposition; at the
20 same time, it acted as a brightener, and produced highly uniform and smooth Ni deposits.
21 ¹⁶ In this study, when NA was used in the Zn electrodeposition, a significant change was
22 observed in the morphology of the Zn film. A bright Zn coating was deposited from
23 *Ethaline* with a concentration of 0.4 M ZnCl₂ and 0.05 M NA. According to the
24 voltammograms of NA in *Ethaline*, as shown in Fig. 4 (a), it can be suggested that NA
25 adsorbs on the cathodic electrode and inhibits the deposition of Zn. An improvement in
26 the smoothness and refinement in the grain size of the Zn deposit, as can be seen in Fig.
27 8 (b), has been obtained as a result of using NA as an additive. Thus, NA can act as a
28 very effective brightener in Zn deposition.
29
30

31 The cross-sectional morphology of the Zn coating deposited from the additive-free
32 electrolyte is shown in Fig. 8 (a). It was found that the Zn coating exhibits good adhesion
33 with the Cu substrate, and the thickness of the coating was uniform with an average value
34 of ~11.1 μm, as based on four thicknesses measured at random positions. A theoretical
35 thickness for Zn film can be calculated based on Faraday's electrolysis law, and was
36 found as 11.67 μm for a deposition current density of 3.3 mA cm⁻². Consequently, the
37 current efficiency was about ~95%, which is close to the efficiency measured from QCM
38 data, Table 1. The cross-sectional morphology of the Zn coating deposited from the
39 electrolyte containing 0.05 M NA is shown in Fig. 8 (b), where small holes were observed
40
41
42
43
44
45
46
47
48
49
50
51
52
53
54
55
56
57
58
59
60
61
62
63
64
65

1 in the cross-sectional morphology of the Zn film. The presence of these holes could
2 correspond to hydrogen evolution occurring on the cathode surface during the
3 electrodeposition process. The thickness of the Zn coating obtained from a system
4 containing NA was increased compared to the above, being found as 15.4 μm , where the
5 recorded increase in film thickness could be attributed to the presence of the small holes
6 in the Zn film.
7
8
9

10
11 Fig. 8 (c) shows photographs, morphologies and cross sections of the Zn deposits
12 obtained from a system containing boric acid. Boric acid is one of the most common
13 compounds to be added to Ni electroplating baths. Researchers have suggested that when
14 boric acid is added to the electroplating bath it acts as a buffering agent to stop or reduce
15 the alkalisation process at the cathodic electrode, which normally occurs due to hydrogen
16 evolution.^{42,49,50} However, several reports in the literature have confirmed that BA acts
17 as a surfactant,⁵⁰ and also that BA interferes with the metal nucleation processes.^{50,51,52}
18 Supicová *et al.*⁵⁰ found that the presence of high concentrations of boric acid in aqueous
19 baths inhibited nickel deposition itself but improved the morphology, brightness, and
20 adhesion of the deposited Ni.
21
22
23
24
25
26
27
28
29

30 In this project, BA was used as a brightener during the electrodeposition of Zn from
31 *Ethaline*. A significant change in the Zn film morphology, where a clear refinement in
32 the grain size of the Zn was obtained, along with a bright Zn film resulting from the use
33 of boric acid, is shown in Fig. 8 (c). Here, BA most likely adsorbs on the electrode
34 surface as a neutral molecule and strongly inhibits the deposition of Zn. The thickness
35 of the Zn deposit was 6.9 μm when the deposition was performed using 0.15 M BA, a
36 significant decrease compared to the thickness of Zn film obtained from the additive-free
37 system. The decrease in the thickness of Zn film in the presence of BA could be due to
38 the adsorption of BA onto the electrode surface, inhibiting the growth of Zn nuclei and
39 enhancing nucleation rate.
40
41
42
43
44
45
46
47
48

49 Fig. 8 (d) shows optical photographs, the morphology and cross sections of the Zn deposit
50 obtained from a system containing 0.03 M BQ. A bright and smooth Zn film was
51 obtained as a result of adding BQ to the Zn electrolyte, and clear refinement in the crystal
52 size of the Zn deposit can be observed in Fig. 8 (d). However, a decrease in the thickness
53 of the Zn film occurred when BQ was used. Here, BQ was thought to be adsorbed on the
54 electrode surface thus inhibiting Zn deposition.
55
56
57
58
59
60
61
62
63
64
65

1
2
3
4
5
6
7
8
9
10
11
12
13
14
15
16
17
18
19
20
21
22
23
24
25
26
27
28
29
30
31
32
33
34
35
36
37
38
39
40
41
42
43
44
45
46
47
48
49
50
51
52
53
54
55
56
57
58
59
60
61
62
63
64
65

Despite the fact that all the coatings were prepared for the same time at the same current density, the observed cross-section thicknesses do not follow the same thickness trend as might be expected based on the current efficiencies, Table 1. This may be because the time over which the QCM mass-charge data were measured over was 8.3 minutes, whereas the bulk deposition was carried out for 2 hrs. This indicates that the current efficiencies deviate at longer time scales perhaps due to bulk, progressive changes in the composition of the electrolyte.

X-ray diffraction

Here, the XRD technique was used to study the crystal orientations of Zn film produced from *Ethaline* in the presence and absence of additives. Fig. 9 shows XRD patterns for the Zn film obtained from *Ethaline* at a concentration of 0.4 M ZnCl₂ in the absence and presence of 0.05 M nicotinic acid, 0.15 M boric acid and 0.03 M *p*-benzoquinone, where all Zn film were achieved on Cu substrate at 80°C, for 2 h at a current density of 3.3 mA cm⁻². XRD patterns of the Zn film obtained from an additive-free system illustrate peaks at 2 Θ = 36.16°, 38.9°, 42.04°, 54.32°, 70.09°, 82.16° and 86.56° which are related to the (002), (100), (101), (102), (103), (112) and (201) planes of hexagonal zinc, respectively.⁵³ The diffraction peaks observed at 2 Θ = 43.2°, 50.4° and 74.14° corresponded to the Cu substrate. It can be seen that the growth of Zn in the additive-free electrolyte preferentially takes place along the (002), (102) and (103) planes.⁵³ However, Zn growth from an electrolyte containing nicotinic acid and boric acid is strongly directed along the (100), (110), (112) and (201) planes where as shown in Fig. 9 and Table. 2. No significant difference was noted in the crystal orientation of Zn film obtained from the system containing *p*-benzoquinone compared to that produced from the Zn electrolyte without any additive.

Bright zinc deposits

Brightness is related to the smoothness surface and its ability to reflect visible light without significant scattering, where roughness should be less than 400 nm. Brightening can be defined as a deposit having crystals of a smaller size than the wavelength of visible light, which on average could be nominally taken to be smaller than 400 nm. Small crystals are essential for brightness, but this in itself is not a satisfactory condition. A

1 number of studies have found that brightness also depends on the orientation of
2 crystallites that are deposited on the surface in the same plane.^{54 47}
3

4 Bright Zn deposits have been obtained when the deposition has been achieved from
5 *Ethaline* with 0.6 M ZnCl₂ and 0.15 M NA. Fig. 10 shows the morphology of a Zn film
6 obtained from *Ethaline* with 0.6 M ZnCl₂ in both the absence and presence of 0.15 M
7 NA, where both experiments were performed at 80°C for 2 h at a current density of 6.15
8 mA cm⁻². As mentioned earlier, NA can be adsorbed on the electrode surface and impede
9 nucleation of large Zn crystals. It is clear from Fig. 10 that a Zn film obtained from a
10 system without additives shows the unorganised deposition of Zn particles in random
11 forms. However, a bright and highly smooth Zn film is produced when electroplating is
12 achieved from *Ethaline* containing 0.6 M ZnCl₂ and 0.15 M of NA.
13
14
15
16
17
18
19
20

21 Earlier we have shown that, a Zn electrodeposit was produced from an electrolyte
22 containing 0.4 M ZnCl₂ with 0.05 M NA at a current density of 3.3 mA cm⁻² and that the
23 addition of NA altered the morphology of the coating (Fig. 8). However, when the
24 concentration of NA was increased (0.6 M ZnCl₂, 0.15 M NA and 5 mA.cm⁻²), a bright,
25 reflective Zn deposit was obtained after cleaning the Zn film surface, Fig. 10. As a
26 consequence, the coating thickness was reduced from 16.17 μm (in the absence of NA)
27 to 11.8 μm in the presence of 0.16 M NA. This may due to a high concentration of NA,
28 allowing its adsorption on the electrode surface and increasing the associated hydrogen
29 evolution, which in turn could lead to a decrease in the thickness and current efficiency
30 of Zn deposition.
31
32
33
34
35
36
37
38
39

40 The roughness and topography of the Zn films obtained from *Ethaline* in the absence and
41 presence of NA were studied using AFM. Fig.10 illustrates the AFM image of a Zn
42 deposit obtained from the electrodeposition of 0.6 M ZnCl₂ in *Ethaline* in the absence
43 and presence of 0.15 M nicotinic acid at 80°C. The roughness of the Zn film obtained
44 from a solution containing NA was about 10 nm; however, the roughness of the Zn film
45 that was achieved from an additive-free solution was about 174 nm.
46
47
48
49
50

51 Cyclic voltammograms of 0.6 M ZnCl₂ in *Ethaline* in the absence and presence of 0.15
52 M NA are shown in Fig.11. The voltammetry was carried out in the potential range 0.0
53 V -1.5 V at a scan rate of 30 mVs⁻¹ using a Pt disc (1 mm diameter) electrode; a Pt flag
54 was used as the counter-electrode, and Ag/AgCl as the reference electrode. In the absence
55 of NA, the onset of Zn reduction (vs. Ag/AgCl) in *Ethaline* was at E = -1.11 V. However,
56
57
58
59
60
61
62
63
64
65

1 this potential was shifted negatively by 15 mV when 0.15 M of NA was added to the Zn
2 solution. Additionally, a significant decrease in the deposition/ dissolution of Zn
3 occurred when NA was added to the Zn electrolyte. NA has been used in the
4 electrodeposition of Ni from DES from which a bright and smooth Ni film was achieved,
5 where it was suggested that NA adsorbed on electrode surface inhibited Ni deposition.²⁸
6 Here, with Zn deposition, it can be similarly suggested that NA adsorbs on electrode
7 surface and inhibits Zn deposition.
8
9

10
11
12
13 Cyclic voltammograms of NA in *Ethaline* were investigated, as shown previously in
14 Fig.4 (a), and NA was deposited at a potential lower than that at of the Zn deposition
15 potential. This means that NA adsorbs on the surface electrode and impedes Zn
16 deposition. In Fig.11, in the presence of NA, a small peak can be observed at -0.47 V
17 which corresponds to the hydrogen evolution that occurs as a result of its reduction. This
18 confirms that NA adsorbs on the electrode surface and inhibits Zn deposition.
19
20
21
22

23
24 XRD patterns of Zn film obtained from Zn solutions in the absence and presence of
25 nicotinic acid are shown in Fig. 12. In the case of the solution without NA, the Zn deposit
26 shows the (002), (100), (101), (102), (103), (112) and (201) orientations and it has been
27 shown that the growth of Zn preferentially takes place along the (002), (101), (102) and
28 (103) planes; however, Zn growth from an electrolyte containing nicotinic acid
29 preferentially take place along the (100) and (110) planes.
30
31
32
33
34
35
36
37
38

39 **Conclusions**

40
41 Organic additives are often added to aqueous electrodeposition baths as levellers and
42 brighteners. However, few studies have considered the effects of additives on the
43 electrodeposition of metals from deep eutectic solvents.
44
45

46
47 In this work, an investigation into the effects of additive addition to the Zn
48 electrodeposition process from *Ethaline* has been presented. The additives studied,
49 nicotinic acid, boric acid and *p*-benzoquinone, have been shown to have varying effects
50 on the Zn deposition. Properties of the Zn electrodeposit have been improved compared
51 to the corresponding system without additives, and for first time a mirror zinc coating has
52 been achieved on a copper substrate when nicotinic acid was used as the additive. It was
53 found that boric acid and *p*-benzoquinone work as brighteners for Zn deposition.
54
55
56
57
58
59
60
61
62
63
64
65

1 Electrochemical experiments, including cyclic voltammetry, chronocoulometry and
2 chronoamperometry, have established a clear difference in Zn electrodeposition
3 processes when the additives were used and in the control experiments where no additive
4 was used. Cyclic voltammetry has shown that these additives may be adsorbed on the
5 electrode surface during the experiment and then inhibit Zn deposition. The
6 morphologies of the Zn deposits using additives were improved compared to the
7 corresponding systems without additives, showing considerable decreases in the
8 roughness of the Zn films obtained when electrodeposition was achieved from a system
9 containing an additive. Decreasing in the current efficiency of Zn deposition occurred
10 when using these additives, especially with NA. In the XRD data shown, the (002), (101)
11 and (102) planes were noted in the crystal orientation of the Zn film obtained from the
12 system without additives. However, Zn growth from an electrolyte containing nicotinic
13 acid and boric acid is strongly directed along the (100), (101) and (110) planes.
14
15
16
17
18
19
20
21
22
23
24
25

26 **Acknowledgements**

27
28
29 HFA wishes to acknowledge the financial support of Ministry of higher education and
30 scientific research in Iraq, HCDDP program is gratefully acknowledged for the studentship
31 to Hasan Alesary. KSR wishes to thank Innovate UK for funding project CRUPPAIL
32 (Cadmium Replacement Using Pulse Plating And Ionic Liquids), project no: 103530.
33
34
35
36
37
38
39
40
41
42
43
44
45
46
47
48
49
50
51
52
53
54
55
56
57
58
59
60
61
62
63
64
65

Table.1: Current efficiencies of Zn deposition from *Ethaline* at a concentration of 0.4 M ZnCl₂ in the absence and presence of 0.05 M NA, 0.15 BA and 0.03 BQ. All experiments were performed on a Pt-coated EQCM crystal at 80°C and at an applied potential of -1.3 V.

ChCl:EG:ZnCl ₂	Cathode Current efficiency %
1:2: 0.4 M Zn	91
1:2: 0.4 M Zn: 0.05 M NA	52
1:2: 0.4 M Zn: 0.15 M BA	71
1:2: 0.4 M Zn: 0.03 M BQ	95

Table. 2: Texture coefficients of the Zn deposits prepared from 1:2 ChCl:EG-based liquid containing 0.4 M ZnCl₂ in the absence and presence of 0.05M nicotinic acid, 0.15 M boric acid and 0.03 M p-benzoquinone. All experiments were performed for 2h at 80°C and at a current density of 3.3 mA cm⁻².

Component	Relative intensity [002]	Relative intensity [100]	Relative intensity [102]	Relative intensity [103]	Relative intensity [112]	Relative intensity [201]
Pure Zn	0.402	0.118	0.154	0.162	0.098	0.064
Zn + NA	0.135	0.269	0.145	0.135	0.155	0.155
Zn + BA	0.152	0.250	0.148	0.147	0.148	0.153
Zn + BQ	0.324	0.150	0.168	0.165	0.101	0.090

1
2
3
4
5
6
7
8
9
10
11
12
13
14
15
16
17
18
19
20
21
22
23
24
25
26
27
28
29
30
31
32
33
34
35
36
37
38
39
40
41
42
43
44
45
46
47
48
49
50
51
52
53
54
55
56
57
58
59
60
61
62
63
64
65

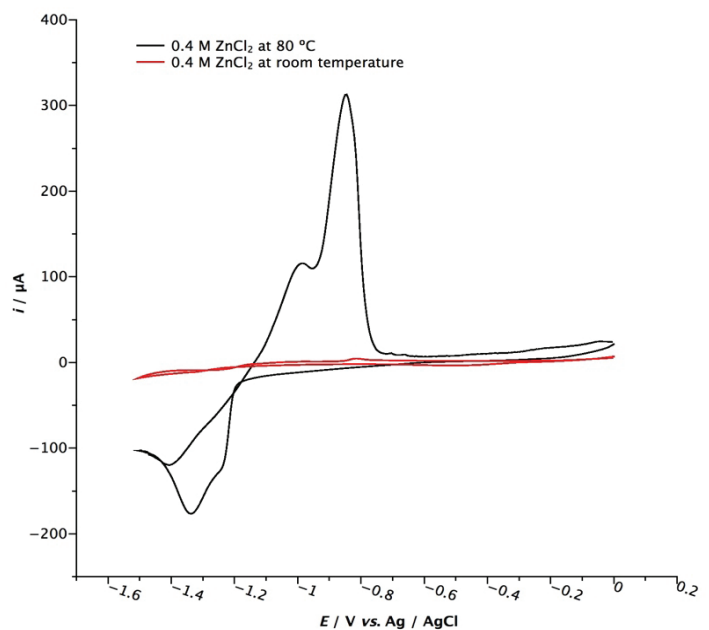


Figure 1: Cyclic voltammograms of 0.4 M ZnCl_2 in *Ethaline* at 80°C (black line) and at room temperature (red line), recorded at a scan rate of 30 mV s^{-1} , using a Pt disc (1 mm diameter) electrode, a Pt flag as the counter-electrode and Ag/AgCl as the reference electrode.

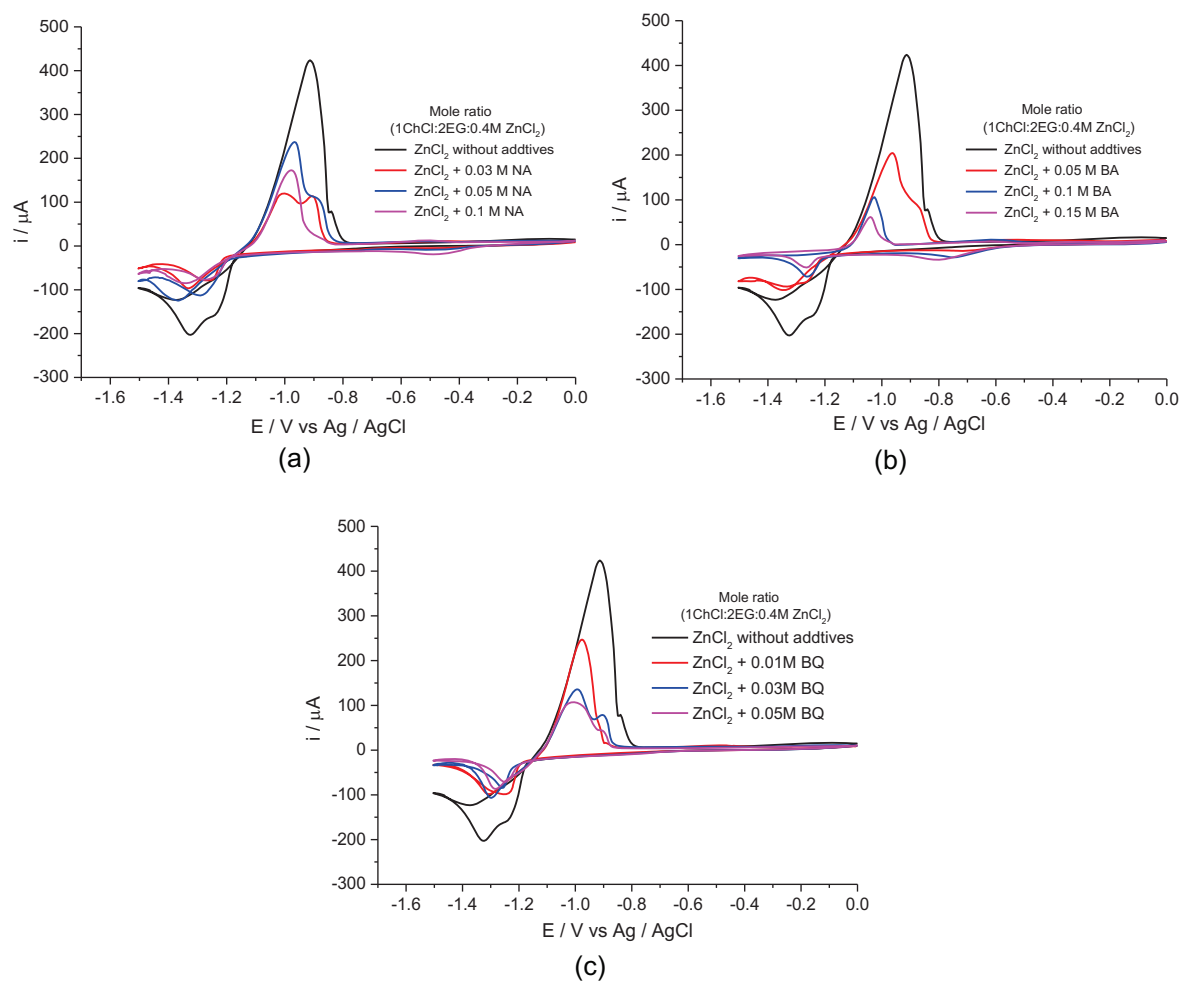


Figure 2: Cyclic voltammograms for 0.4 M $ZnCl_2$ obtained from *Ethaline*, using a Pt disc electrode (1 mm diameter) at $80^\circ C$ and at a scan rate of 30 mV s^{-1} with the following organic additives: (a) nicotinic acid, (b) boric acid, and (c) p-benzoquinone.

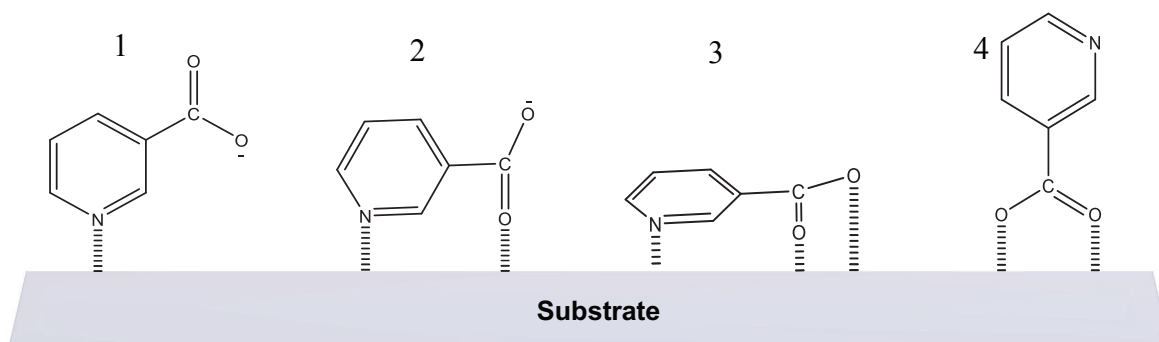


Figure 3: The orientation and probability of molecular adsorption of nicotinic acid.

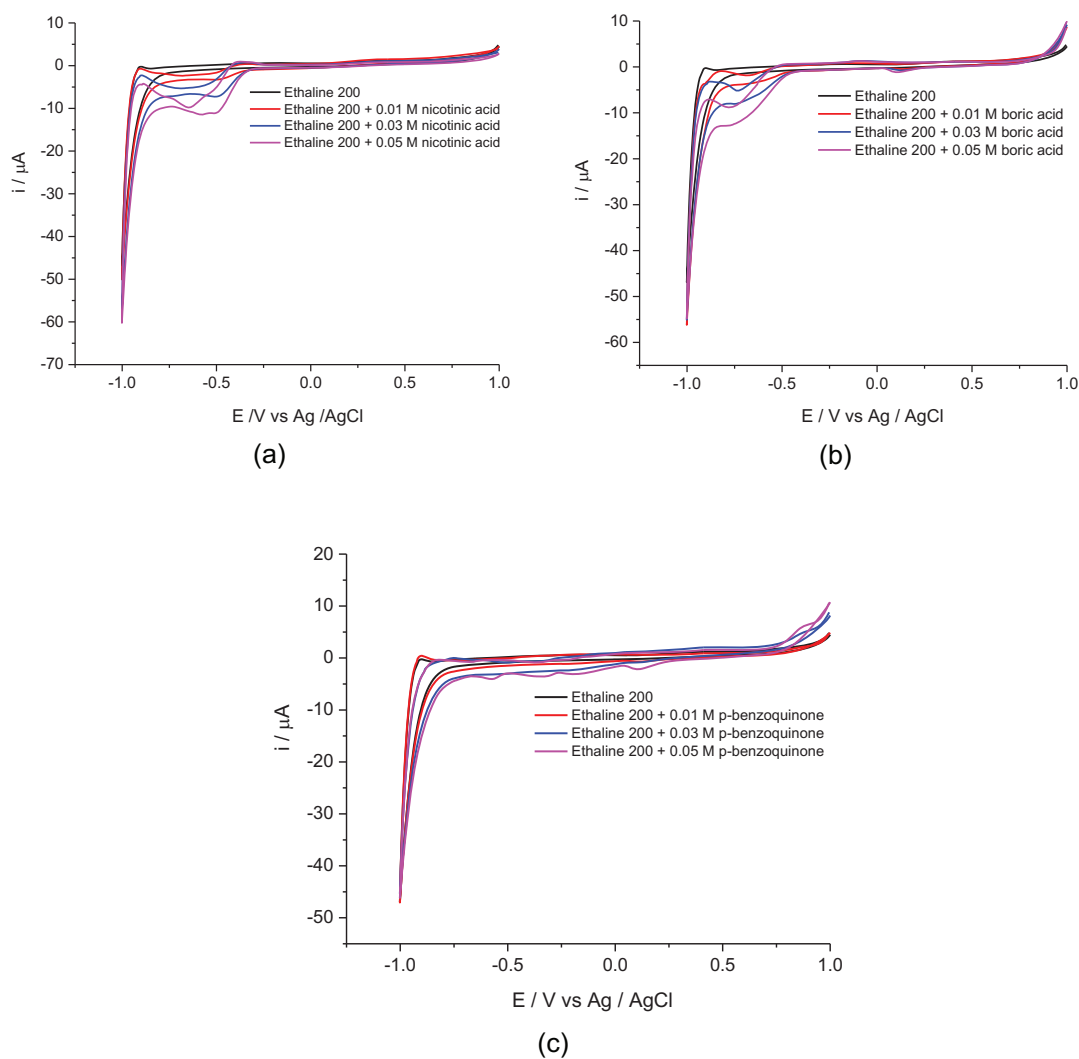


Figure 4: Cyclic voltammogram at 80 °C of *Ethaline* with varying amounts of (a) NA, (b) BH and (c) BQ. Measured using a 1 mm Pt disc working electrode, Pt flag counter electrode and reference against Ag / AgCl at 10 mV s⁻¹.

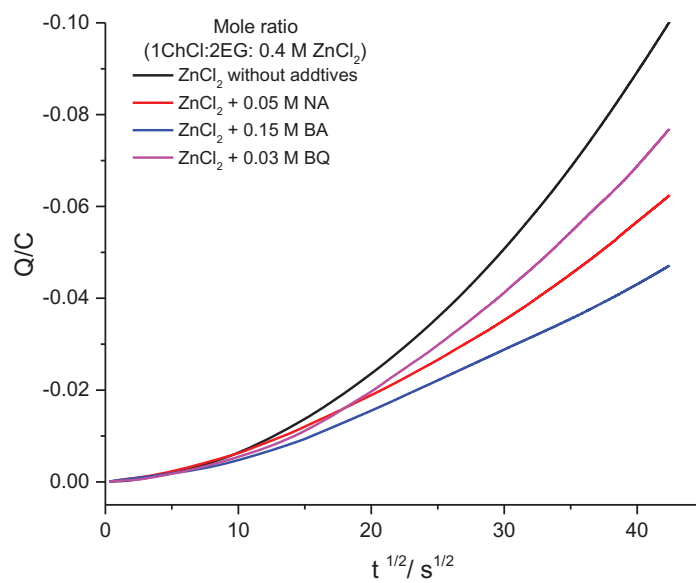


Figure 5: Chronocoulometry of 0.4 M [ZnCl₂] in *Ethaline* in the absence and presence of 0.05 M NA, 0.2 M BA and 0.03 M BQ. All experiments were achieved at a potential of -1.3 V for 1800 s on Pt (1.0 mm diam) and at 80°C.

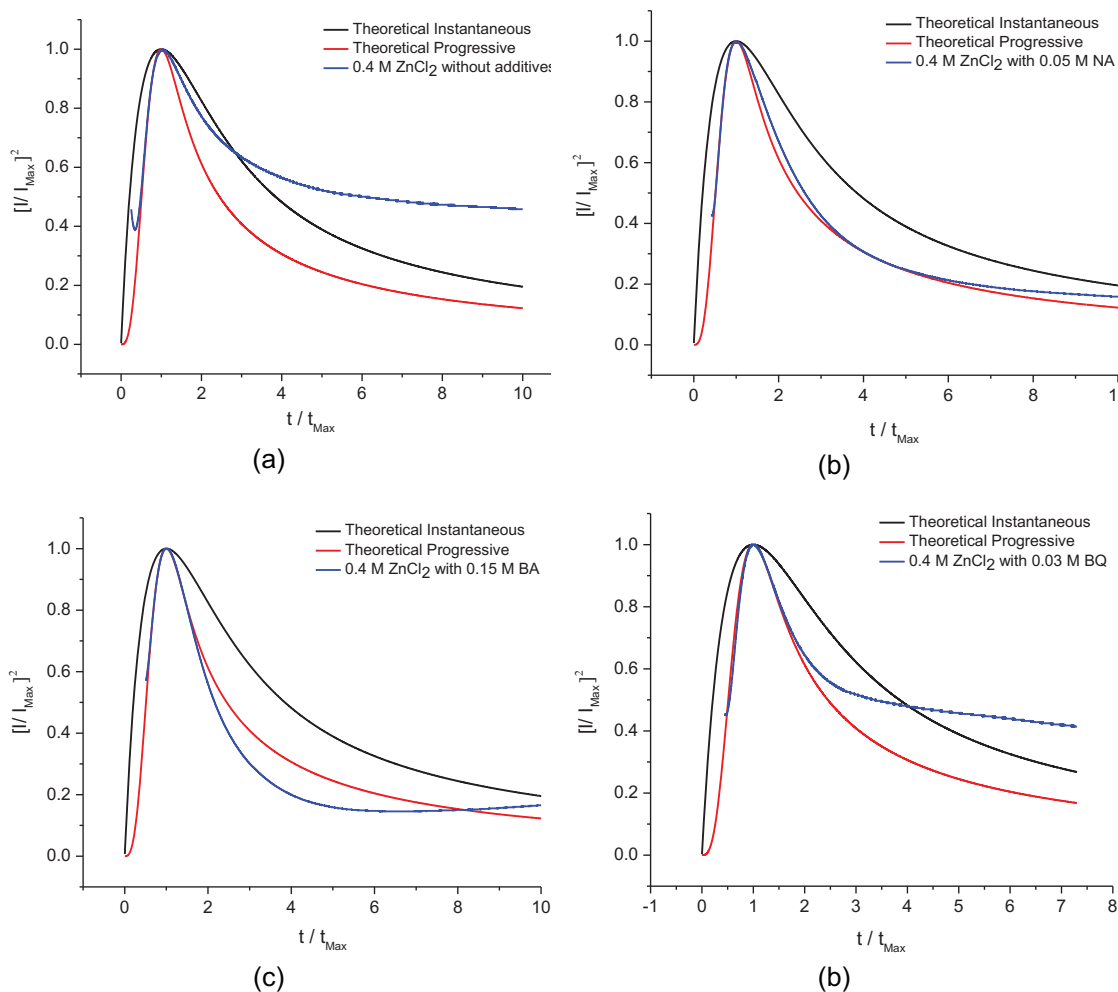


Figure 6: The experimental i - t data for electrodeposition of 0.4 M ZnCl₂ from *Ethaline* on a Pt disc (1 mm diameter) at 80°C vs. an Ag/AgCl reference electrode in the absence and presence of additives: (a) without additives; (b) 0.05 M NA; (c) 0.15 M BA; and (d) 0.03 M BQ. The applied potential was -1.25 V for all experiments.

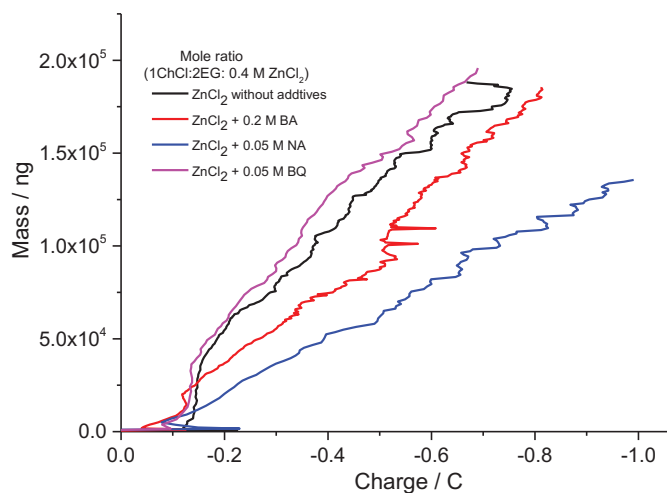


Figure 7: Gravimetric EQCM traces for Zn metal deposition on a Pt-coated quartz crystal (10 MHz) surface in mass vs. charge. All experiments were performed in *Ethaline* at a concentration of 0.4 M ZnCl₂ at 80 °C in the presence and absence of additives. The applied potential was -1.3 V vs. Ag/AgCl for 500 s.

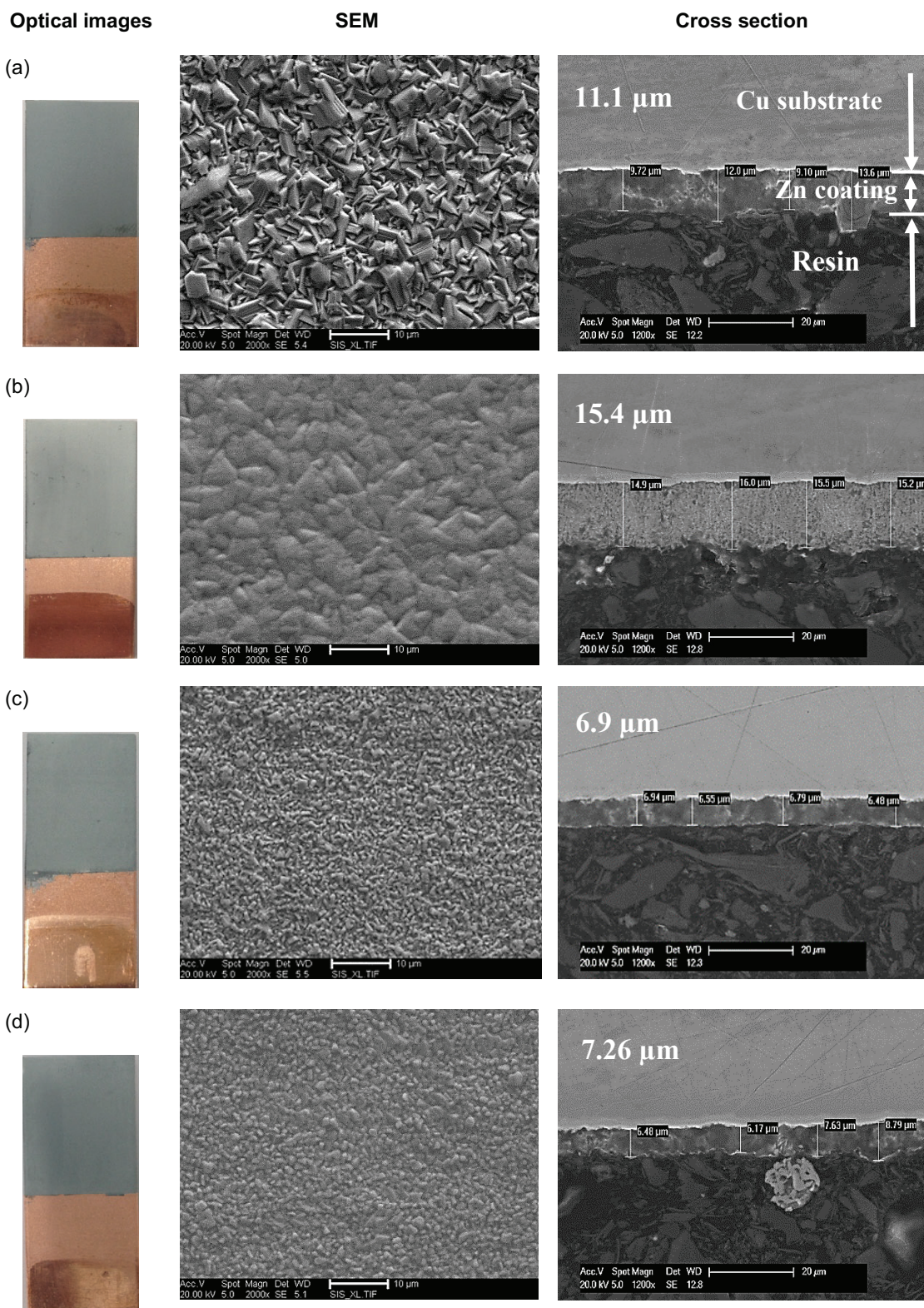


Figure 8: Optical photographs and SEM images with cross-sectional samples after bulk electrodeposition from *Ethaline* systems containing 0.4 M ZnCl_2 using following additives: (a) without additives; (b) 0.05 M NA; (c) 0.2 M BA; and (d) 0.03 M BQ. (All experiments were performed at 80°C for 2 h on a Cu electrode with an applied current density of 3.3 mA cm^{-2}).

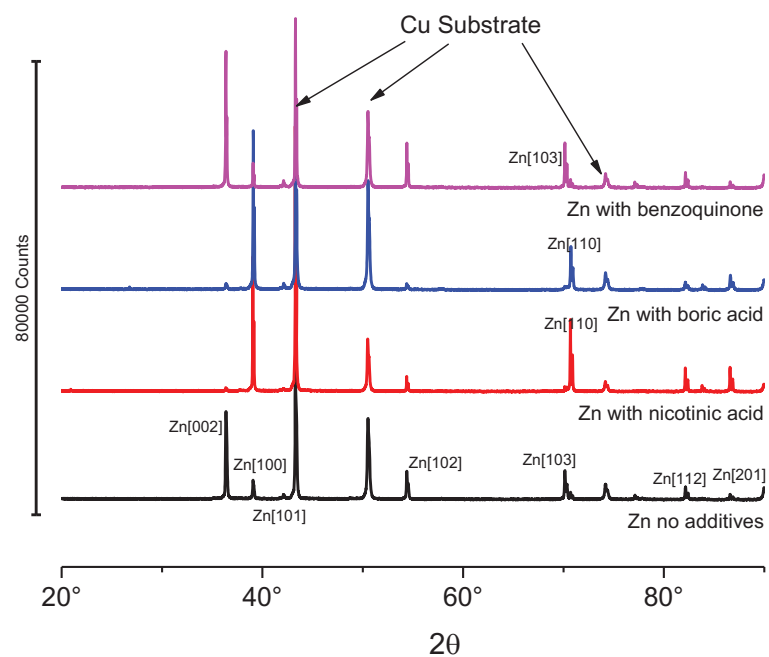


Figure 9: XRD patterns for Zn deposits from 0.4 M $ZnCl_2$ in *Ethaline* with the following organic additives: 0.05M nicotinic acid, 0.15 M boric acid and 0.03 M p-benzoquinone. All experiments were performed for 2 h at 80°C and at a current density of 3.3 mA cm⁻².

1
2
3
4
5
6
7
8
9
10
11
12
13
14
15
16
17
18
19
20
21
22
23
24
25
26
27
28
29
30
31
32
33
34
35
36
37
38
39
40
41
42
43
44
45
46
47
48
49
50
51
52
53
54
55
56
57
58
59
60
61
62
63
64
65

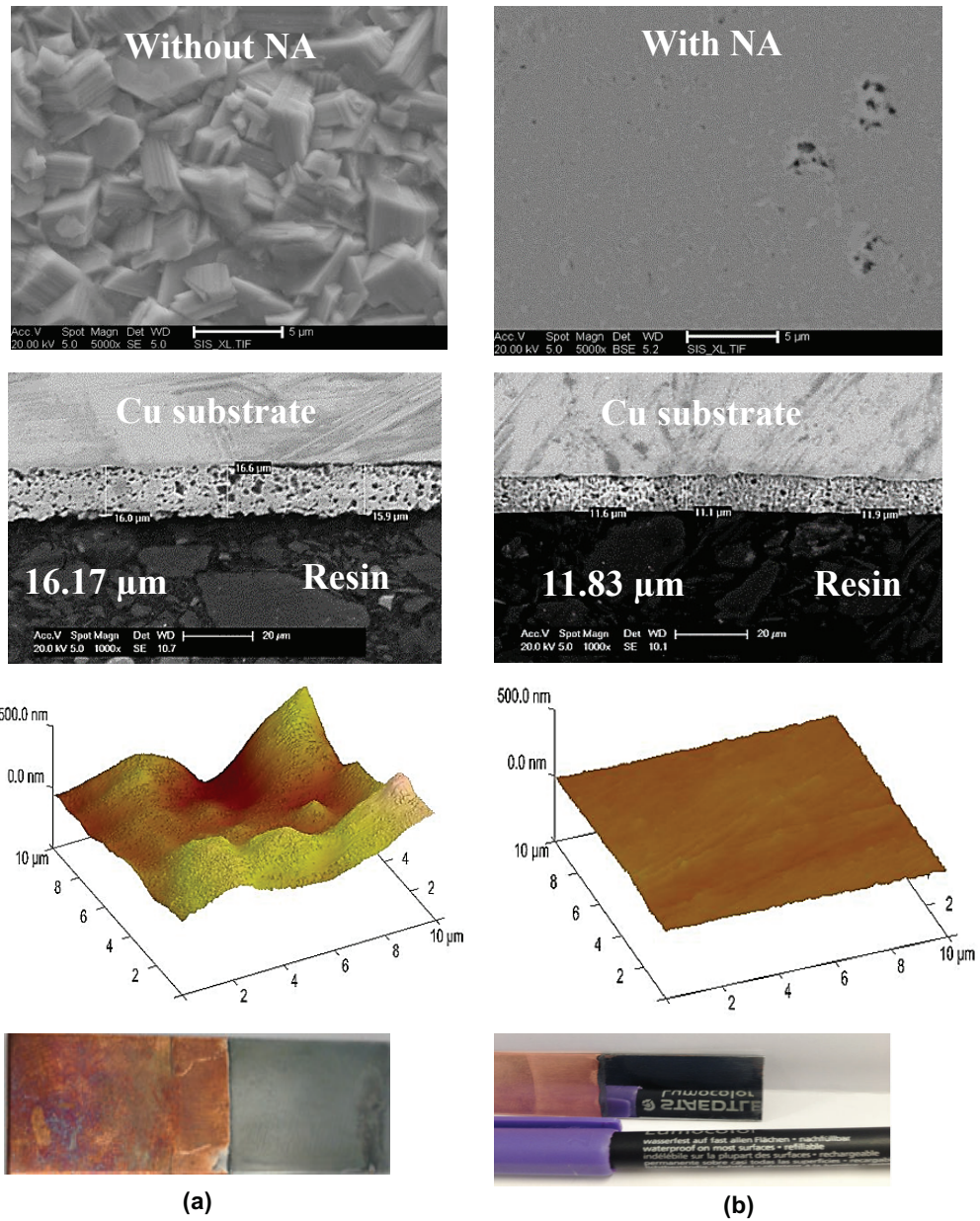


Figure 10: Morphologies and AFM images of Zn films obtained from *Ethaline* in the absence and presence of NA, (a) without NA and (b) with NA. (the deposition was achieved from *Ethaline* with 0.6 M ZnCl₂, with and without 0.15 M NA, at a current density of 5 mA cm⁻² for 2 h on a Cu substrate at 80°C.

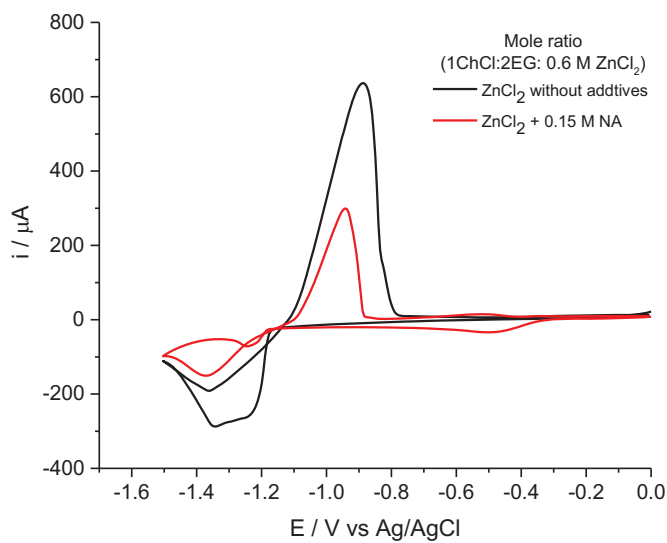


Figure 11: Cyclic voltammograms of 0.6 M ZnCl_2 in *Ethaline* in the absence and presence of 0.15 M nicotinic acid using a Pt disc (1 mm diameter) electrode, a Pt flag counter electrode and Ag/AgCl as the reference electrode at 30 mVs^{-1} and 80°C .

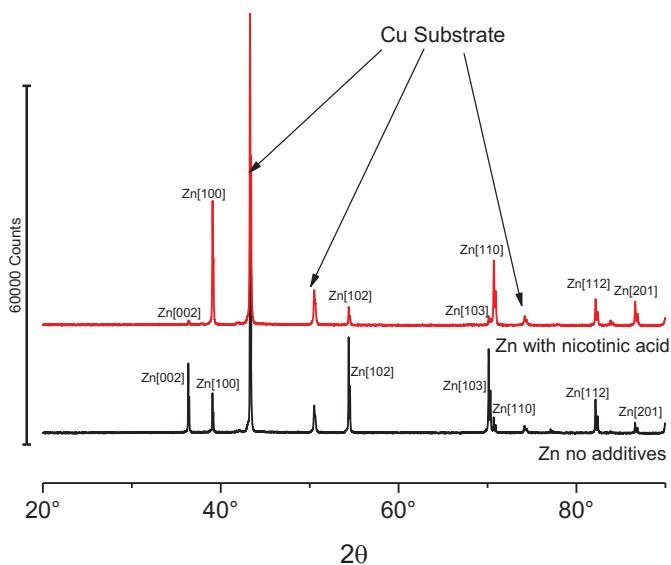


Figure 12: XRD patterns for Zn deposits from 0.6 M ZnCl_2 in *Ethaline* in the absence and presence of 0.15 M nicotinic acid, 0.15 M boric acid and 0.03 M p-benzoquinone. All experiments were performed for 2 h at 80°C and at a current density of 6.5 mA cm^{-2} .

References

- 1 A. P. Abbott, J. C. Barron, G. Frisch, K. S. Ryder and A. F. Silva, *Electrochimica Acta*, 2011, **56**, 5272-5279
- 2 F. Endres, D. MacFarlane and A. Abbott, *Electrodeposition from ionic liquids*, John Wiley & Sons 2008
- 3 G. H. Lane, A. S. Best, D. R. MacFarlane, M. Forsyth and A. F. Hollenkamp, *Electrochimica Acta*, 2010, **55**, 2210-2215.
- 4 S. Ibrahim, A. Bakkar, E. Ahmed and A. Selim, *Electrochimica Acta*, 2016, **191**, 724-732.
- 5 S. Müller, F. Holzer and O. Haas, *Journal of Applied Electrochemistry*, 1998, **28**, 895-898.
- 6 X. Zhai, C. Sun, K. Li, M. Agievich, J. Duan and B. Hou, *Journal of Industrial and Engineering Chemistry*, 2016, **36**, 147-153.
- 7 R. Krishnan, S. Natarajan, V. Muralidharan and G. Singh, *Plating and Surface Finishing*, 1992, **79**, 67-70.
- 8 M. Pushpavanam, *Journal of Applied Electrochemistry*, 2006, **36**, 315-322.
- 9 Q. Zhang, K. D. O. Vigier, S. Royer and F. Jérôme, *Chemical Society Reviews*, 2012, **41**, 7108-7146.
- 10 L. Vieira, R. Schennach and B. Gollas, *Electrochimica Acta*, 2016, **197**, 344-352.
- 11 A. P. Abbott, D. Boothby, G. Capper, D. L. Davies and R. K. Rasheed, *Journal of the American Chemical Society*, 2004, **126**, 9142-9147.
- 12 A. Paiva, R. Craveiro, I. Aroso, M. Martins, R. L. Reis and A. R. C. Duarte, *ACS Sustainable Chemistry & Engineering*, 2014, **2**, 1063-1071.
- 13 K. Haerens, E. Matthijs, A. Chmielarz and B. Van der Bruggen, *Journal of Environmental Management*, 2009, **90**, 3245-3252.
- 14 N. M. Pereira, P. M. Fernandes, C. M. Pereira and A. F. Silva, *Journal of The Electrochemical Society*, 2012, **159**, D501-D506.
- 15 M. Hayyan, M. A. Hashim, A. Hayyan, M. A. Al-Saadi, I. M. AlNashef, M. E. Mirghani and O. K. Saheed, *Chemosphere*, 2013, **90**, 2193-2195.
- 16 E. L. Smith, A. P. Abbott and K. S. Ryder, *Chemical Reviews*, 2014, **114**, 11060-11082.
- 17 A. P. Abbott, K. El Ttaib, G. Frisch, K. J. McKenzie and K. S. Ryder, *Phys. Chem. Chem. Phys.*, 2009, **11**, 4269-4277.
- 18 J. C. Barron, PhD thesis, University of Leicester, **2010**.
- 19 G. Trejo, H. Ruiz, R. O. Borges and Y. Meas, *Journal of Applied Electrochemistry*, 2001, **31**, 685-692.
- 20 J.-Y. Lee, J.-W. Kim, M.-K. Lee, H.-J. Shin, H.-T. Kim and S.-M. Park, *Journal of the Electrochemical Society*, 2004, **151**, C25-C31.
- 21 J. J. Kelly, C. Tian and A. C. West, *Journal of the Electrochemical Society*, 1999, **146**, 2540-2545.
- 22 T. Iwagishi, H. Yamamoto, K. Koyama, H. Shirai and H. Kobayashi, *Electrochemistry*, 2002, **70**, 671-674.
- 23 K. Koyama, T. Iwagishi, H. Yamamoto, H. Shirai and H. Kobayashi, *Electrochemistry (Japan)*, 2002, **70**, 178-182.
- 24 A. P. Abbott and K. J. McKenzie, *Physical Chem. Chem. Phys.*, 2006, **8**, 4265-4279.
- 25 F. Endres, M. Bukowski, R. Hempelmann and H. Natter, *Angewandte Chemie International Edition*, 2003, **42**, 3428-3430.
- 26 Z. Liu, S. Z. El Abedin and F. Endres, *Electrochimica Acta*, 2013, **89**, 635-643.

-
- 1 27 P.-Y. Chen and I.-W. Sun, *Electrochimica Acta*, 2001, **46**, 1169-1177.
2
3 28 H. Yang, X. Guo, N. Birbilis, G. Wu and W. Ding, *Applied Surface Science*, 2011, **257**,
4 9094-9102.
5 29 A. P. Abbott, A. Ballantyne, R. C. Harris, J. A. Juma and K. S. Ryder, *Phys. Chem.*
6 *Chem., Phys.*, 2017, **19**, 3219.
7 30 A. P. Abbott, J. C. Barron, G. Frisch, S. Gurman, K. S. Ryder and A. F. Silva, *Phys.*
8 *Chem. Chem. Phys.*, 2011, **13**, 10224-10231.
9 31 J. Juma, PhD thesis, University of Leicester, 2017.
10 32 Andrew P. Abbott, John C. Barron, Karl S. Ryder and Emma L. Smith, *Anal. Chem.*,
11 2009, **81**, 8466-8471.
12 33 Andrew P. Abbott, John C. Barron and Karl S. Ryder, *Trans. IMF*, 2009, **87**, 201-207.
13 34 J. L. Ortiz-Aparicio, Y. Meas, G. Trejo, R. Ortega, T. W. Chapman and E. Chainet,
14 *Journal of Applied Electrochemistry*, 2013, **43**, 289-300.
15 35 J. Barthelmes, G. Pofahl and W. Plieth, *J. Electroanal. Chem.*, 1993, **349**, 223-231.
16 36 N. Batina, D. G. Frank, J. Y. Gui, B. E. Kahn, C.-H. Lin, F. Lu, J. W. McCargar, G. N.
17 Salaita, D. A. Stern and D. C. Zapien, *Electrochimica Acta*, 1989, **34**, 1031-1044.
18 37 J. Y. Gui, B. E. Kahn, L. Laguren-Davidson, C. H. Lin, F. Lu, G. N. Salaita, D. A. Stern
19 and A. T. Hubbard, *Langmuir*, 1989, **5**, 819-828.
20 38 N. Zech and D. Landolt, *Electrochimica Acta*, 2000, **45**, 3461-3471.
21 39 J. Horkans, *Journal of the Electrochemical Society*, 1979, **126**, 1861-1867.
22 40 X. Wang, N. Yang and Q. Wan, *Electrochimica acta*, 2006, **52**, 361-368.
23 41 A. El-Shafei and A. Aramata, *Journal of Solid State Electrochemistry*, 2007, **11**, 430-433.
24 42 C. Davalos, J. Lopez, H. Ruiz, A. Méndez, R. Antano-Lopez and G. Trejo, *Int J*
25 *Electrochem Sci*, 2013, **8**, 9785.
26 43 A. I. Alhaji, PhD thesis, University of Leicester, 2012.
27 44 B. Scharifker and G. Hills, *Electrochimica Acta*, 1983, **28**, 879-889.
28 45 G. Gunawardena, G. Hills and I. Montenegro, *Journal of Electroanalytical Chemistry*
29 *and Interfacial Electrochemistry*, 1985, **184**, 371-389.
30 46 G. Gunawardena, G. Hills, I. Montenegro and B. Scharifker, *Journal of Electroanalytical*
31 *Chemistry and Interfacial Electrochemistry*, 1982, **138**, 225-239.
32 47 M. S. Cruz, F. Alonso and J. Palacios, *Journal of Applied Electrochemistry*, 1993, **23**,
33 364-370.
34 48 G. Sauerbrey, *Z. Phys.*, 1959, **155**, 202.
35 49 J. Ji, W. Cooper, D. Dreisinger and E. Peters, *Journal of Applied Electrochemistry*, 1995,
36 **25**, 642-650.
37 50 M. Šupicová, R. Rozik, L. Trnková, R. Oriňáková and M. Gálová, *Journal of Solid State*
38 *Electrochemistry*, 2006, **10**, 61-68.
39 51 C. Karwas and T. Hepel, *Journal of the Electrochemical Society*, 1988, **135**, 839-844.
40 52 C. Karwas and T. Hepel, *Journal of the Electrochemical Society*, 1989, **136**, 1672-1678.
41 53 M. S. Ghazvini, G. Pulletikurthi, A. Lahiri and F. Endres, *ChemElectroChem*, 2016, **3**,
42 598-604.
43 54 L. Oniciu and L. Mureşan, *Journal of Applied Electrochemistry*, 1991, **21**, 565-574.
44
45
46
47
48
49
50
51
52
53
54
55
56
57
58
59
60
61
62
63
64
65